

Supplementary Information

The activity key of s-Block Single-Atom Catalysts for Superior CO₂RR: sp² Hybridization of metal sites

Ce Liu^a, Shoufu Cao^b, Yuteng Wei^a, Zengxuan Chen^a, Siyuan Liu^a, Hongyu Chen^a,
Yitong Yin^a, Shaolong Yue^a, Shuxian Wei^c, Zhaojie Wang^{a*}, Xiaoqing Lu^a

^a *School of Materials Science and Engineering, China University of Petroleum, Qingdao, Shandong 266580, P. R. China*

^b *Department of Chemistry and Guangdong Provincial Key Laboratory of Catalysis, Southern University of Science and Technology, Shenzhen 518055 Guangdong, China*

^c *College of Science, China University of Petroleum, Qingdao, Shandong 266580, P. R. China*

* Corresponding authors: Zhaojie Wang

E-mail address: wangzhaojie@upc.edu.cn

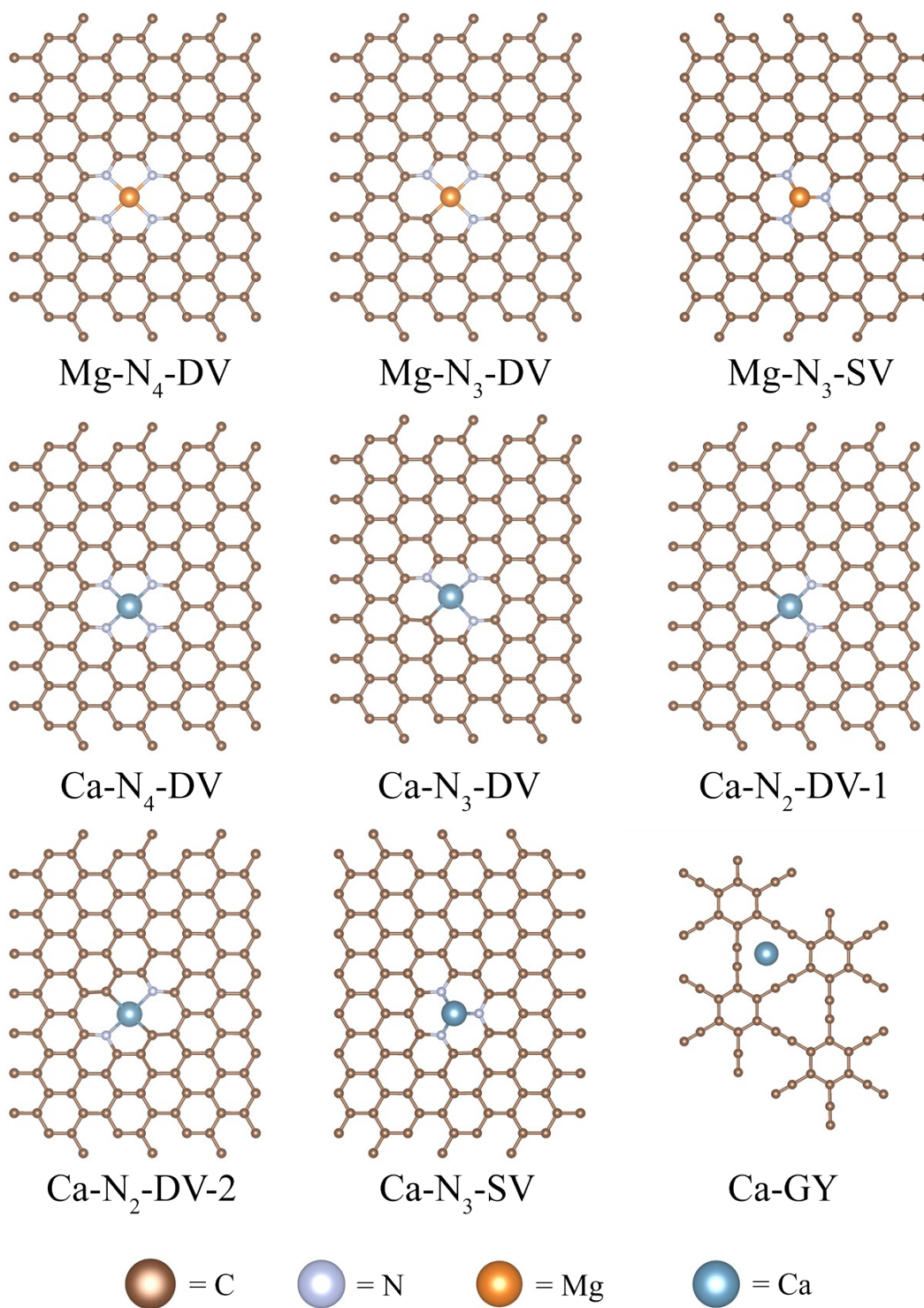


Figure S1 Structural diagrams of all stabilized structures

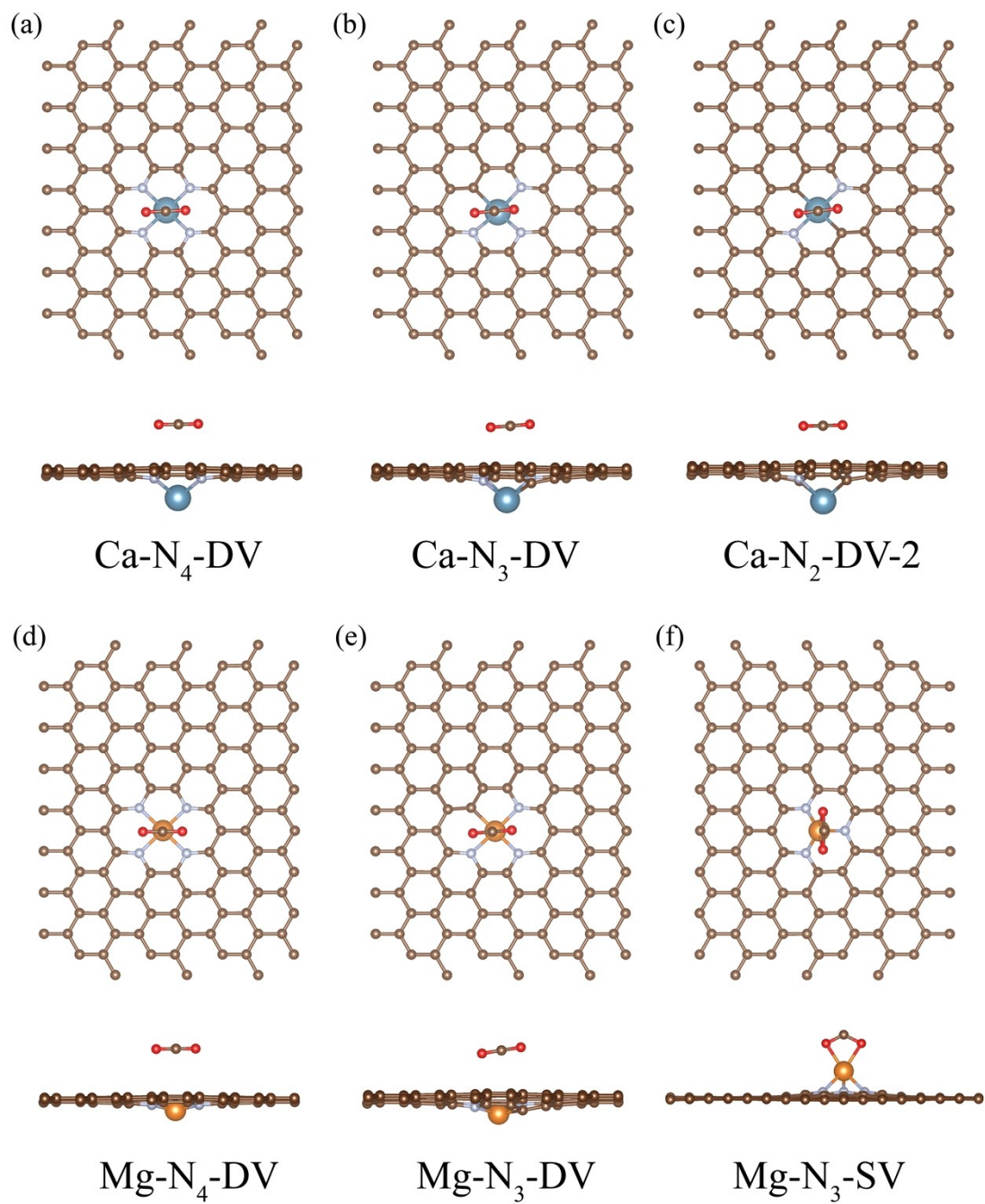


Figure S2 Top and side views of CO_2 adsorbed on (a) $\text{Ca-N}_4\text{-DV}$, (b) $\text{Ca-N}_3\text{-DV}$, (c) $\text{Ca-N}_2\text{-DV-2}$, (d) $\text{Mg-N}_4\text{-DV}$, (e) $\text{Mg-N}_3\text{-DV}$ and (f) $\text{Mg-N}_3\text{-SV}$

In-depth discussion on adsorption mechanisms

By analyzing geometric data, Bader charge distribution, charge density difference maps, and partial density of states (pDOS), we found that CO₂ adsorption on Ca-N₂-DV-1 is primarily physisorption, whereas on Ca-N₃-SV and Ca-GY, it exhibits chemisorption characteristics. While chemisorption is typically associated with a more negative adsorption energy, promoting catalytic reactions, our study reveals an intriguing observation. In our work, the chemisorption of CO₂ on our s-block signal-atom catalysts exhibits a substantial free energy barrier (~2 eV), which significantly impedes the CO₂ reduction reaction (CO₂RR). To understand the origins of this phenomenon, we conducted an in-depth investigation.

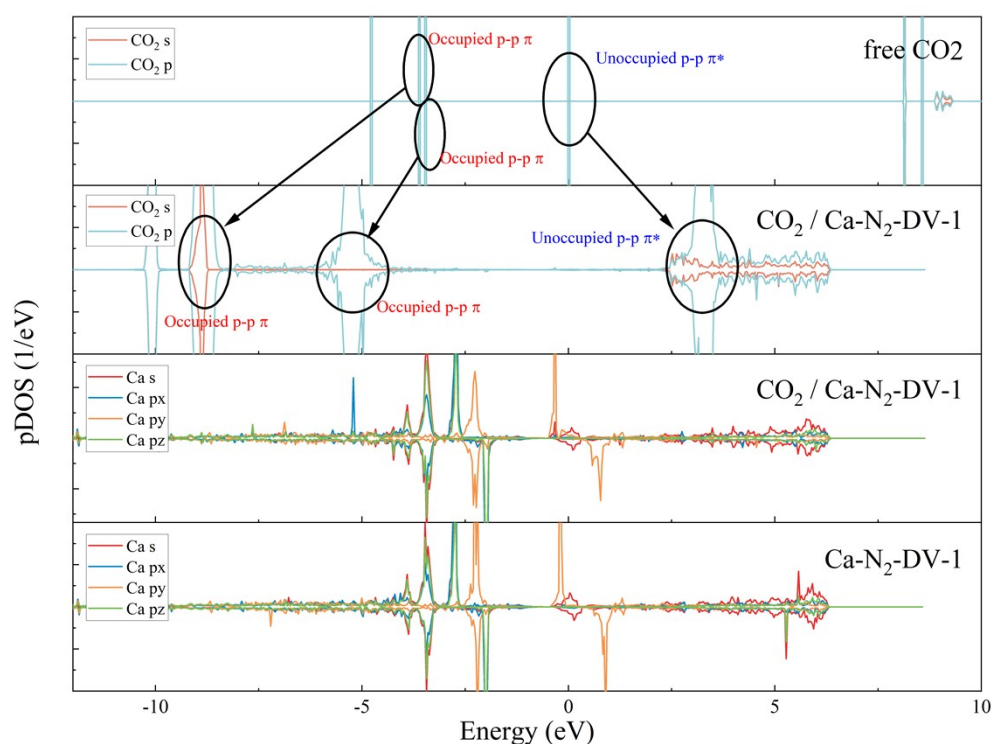


Figure S3 pDOS of free bent CO₂, CO₂ adsorbed on Ca-N₂-DV-1 and Ca-N₂-DV-1.

Figure S3 illustrates the detailed process of CO₂ physisorption on Ca-N₂-DV-1. Notably, following physisorption, the energy levels of the orbitals undergo changes, becoming more delocalized. However, despite these alterations, the filling of the

orbitals remains unchanged, and no additional bonding was observed.

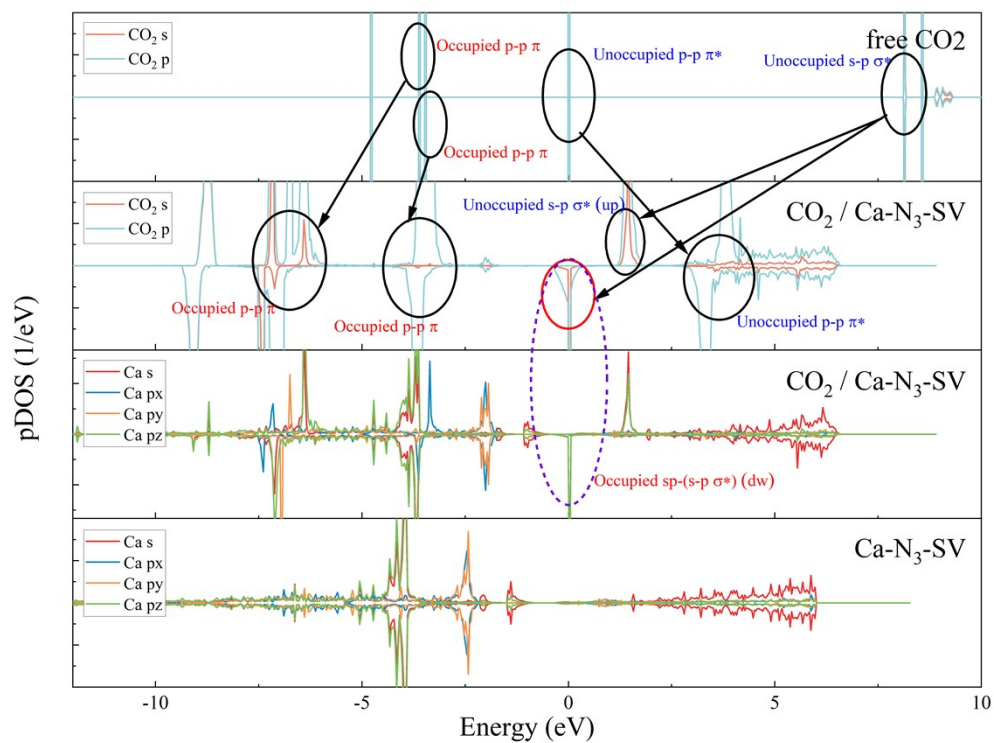


Figure S4 pDOS of free bent CO₂, CO₂ adsorbed on Ca-N₃-SV and Ca-N₃-SV.

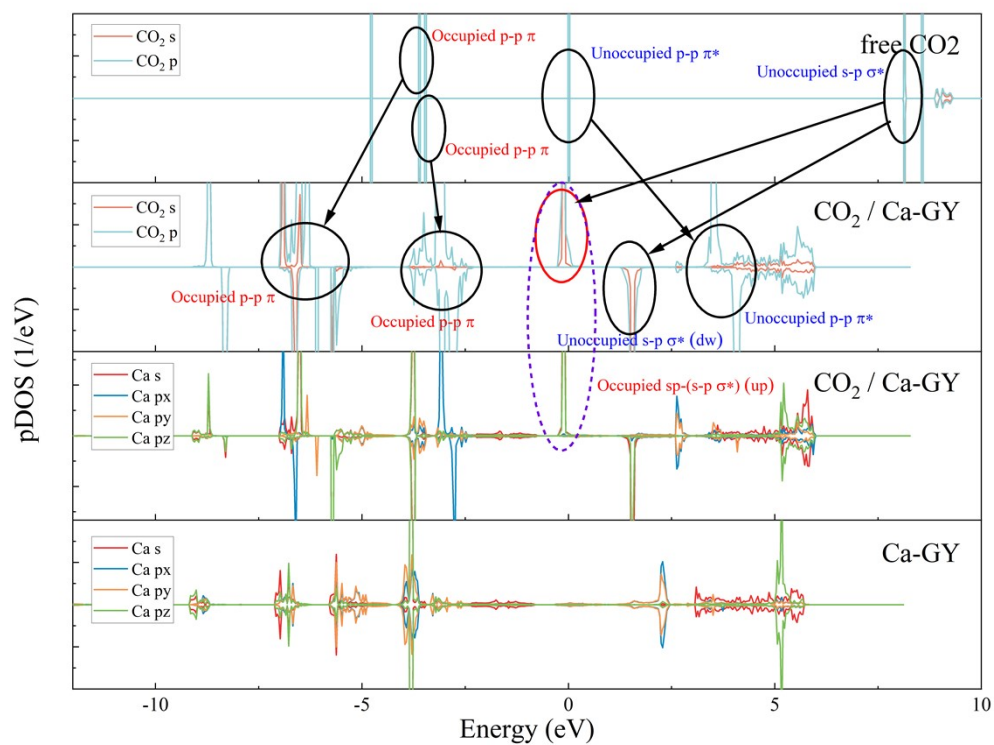


Figure S5 pDOS of free bent CO₂, CO₂ adsorbed on Ca-GY and Ca-GY.

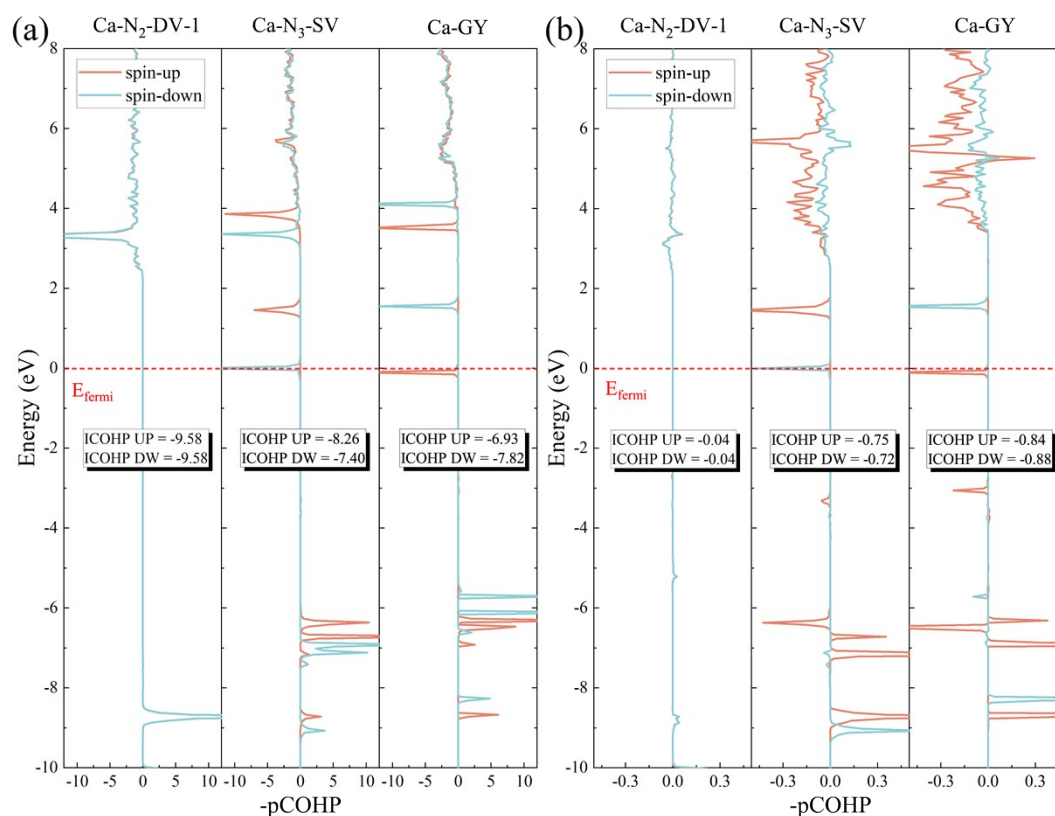


Figure S6 The projected Crystal Orbital Hamilton Populations (pCOHP) and integrated pCOHP (ICOHP) values of (a) C-O bonds and (b) Ca-O bonds on Ca-N₂-DV-1, Ca-N₃-SV, and Ca-GY.

Figure S4 provides a detailed depiction of the CO₂ chemisorption process on Ca-N₃-SV. Notably, the s-p σ orbital, formed by the C 2p and O 2p orbitals, weakly interacts with the Ca sp hybridized orbital. As a result, occupied sp- σ bonding orbitals form, exhibiting weak bonding characteristics (Figure S6b^{1,2}). Additionally, the degenerate p-p π orbitals, formed by the C 2p and O 2p orbitals, interact with the Ca sp hybridized orbital. Specifically, they give rise to occupied sp- π bonding orbitals and (sp- π)* antibonding orbitals. These orbitals contribute to bonding and antibonding interactions (Figure S6b), with offsetting effects on the overall energy. Additionally, the σ antibonding orbital formed by C 2s and O 2p bond to Ca sp hybridized orbital with matching symmetry. This interaction results in the formation of unoccupied sp- σ * antibonding orbitals (spin-up) and occupied sp- σ * antibonding orbitals (spin-down). Notably, the substantial energy level difference between the C 2s and O 2p orbitals

leads to the creation of a σ antibonding orbital with pronounced antibonding properties. Consequently, the presence of occupied $sp-\sigma^*$ antibonding orbitals (spin-down) significantly increases the system energy (Figure S6a, b).

Figure S5 illustrates the detailed process of CO_2 chemisorption on Ca-GY. Notably, this process closely resembles that observed for Ca-N₃-SV.

In summary, CO_2 does not form bonds with Ca-N₂-DV-1 due to the absence of matching symmetry, resulting in smaller free energy changes before and after adsorption. However, certain bonding and antibonding molecular orbitals of CO_2 interact with Ca sp hybridized orbitals with matching symmetry, resulting in bonding and antibonding interactions. While the partial bonding state reduces the total energy, the occupation of the strong antibonding orbital σ^* significantly elevates the overall energy, leading to a substantial CO_2 chemisorption barrier.

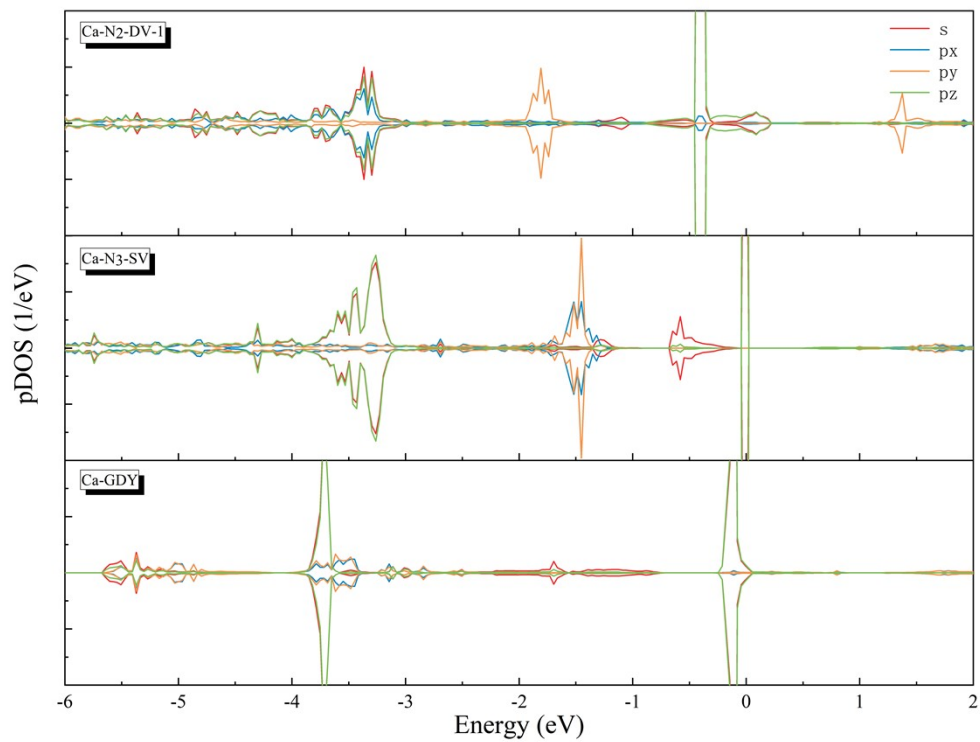


Figure S7 pDOS of H adsorbed on Ca-N₂-DV-1, Ca-N₃-SV and Ca-GY.

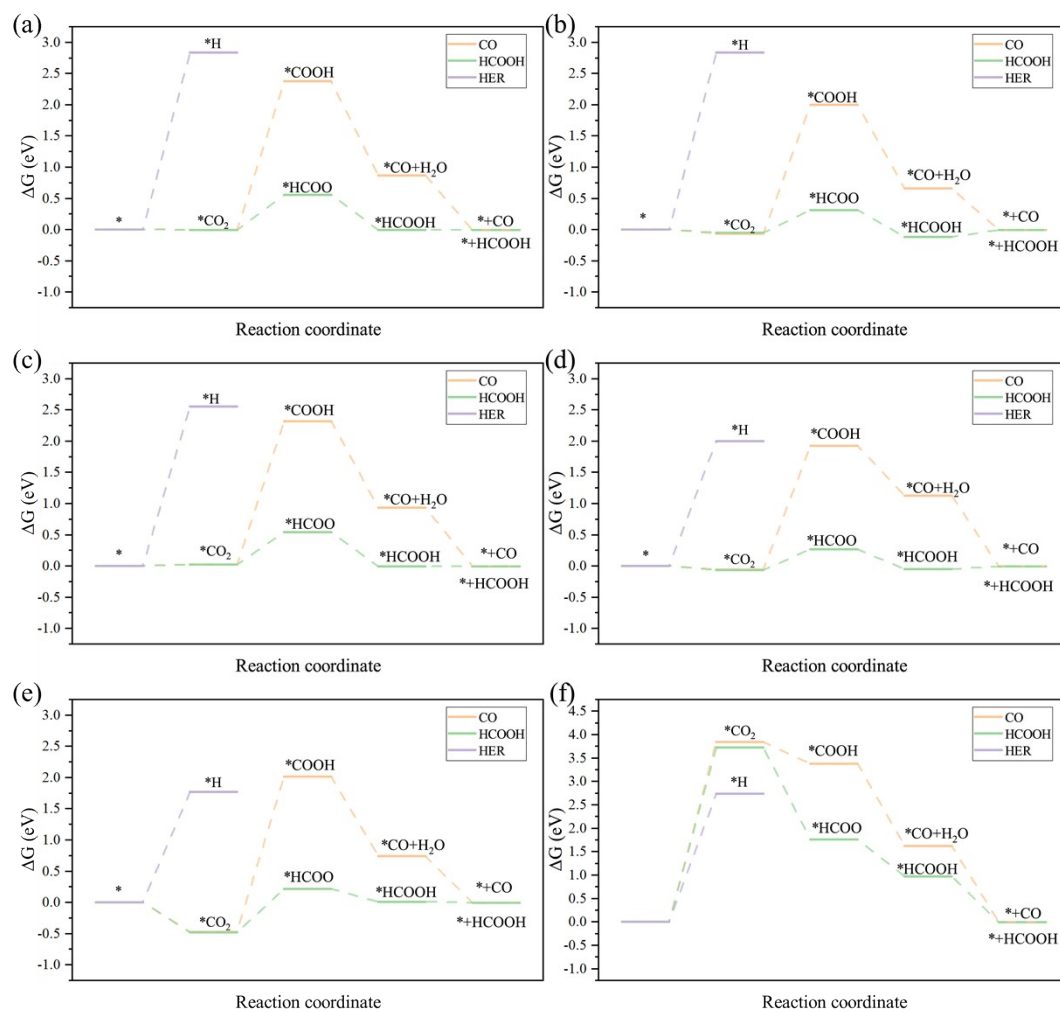


Figure S8 The constant Potential free energy diagrams for CO₂RR and HER on (a) Ca-N₄-DV, (b) Ca-N₂-DV-2, (c) Ca-N₃-DV, (d) Mg-N₄-DV, (e) Mg-N₃-DV and (f) Mg-N₃-SV at equilibrium potentials.

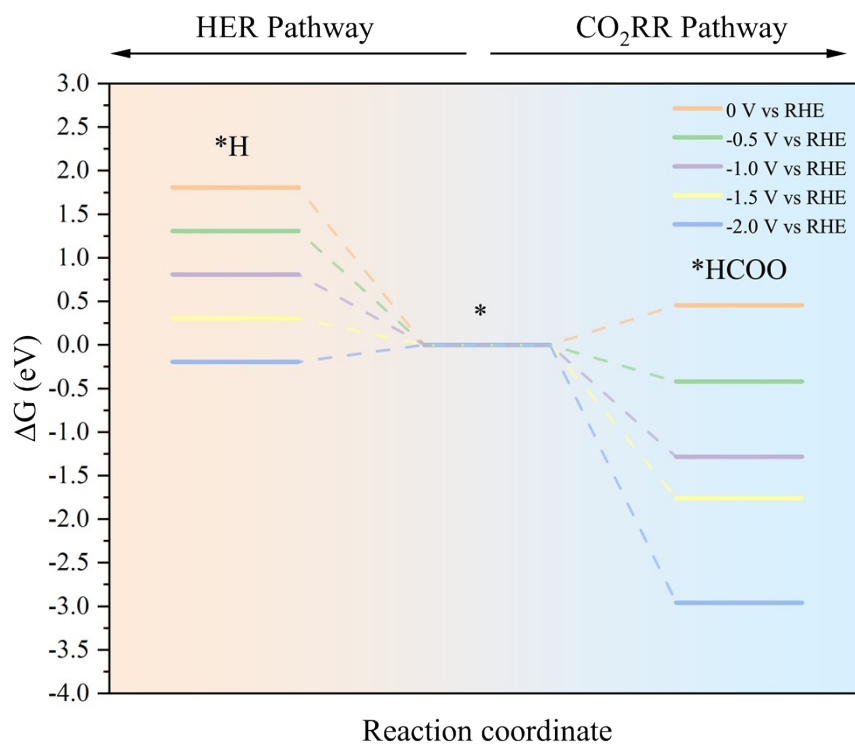


Figure S9 The constant Potential free energy diagrams for the first hydrogenation step with applied potential on Ca-N₂-DV-1.

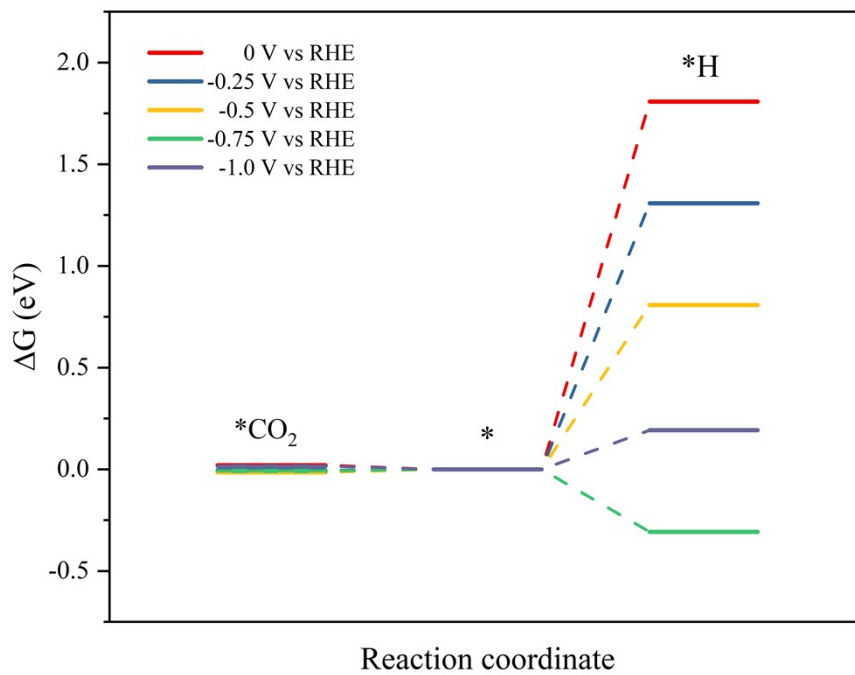


Figure S10 The constant Potential free energy diagrams of CO_2 and H adsorption under varying applied potentials (0 V, -0.25 V, -0.5 V, -0.75 V, -1.0 V vs RHE).

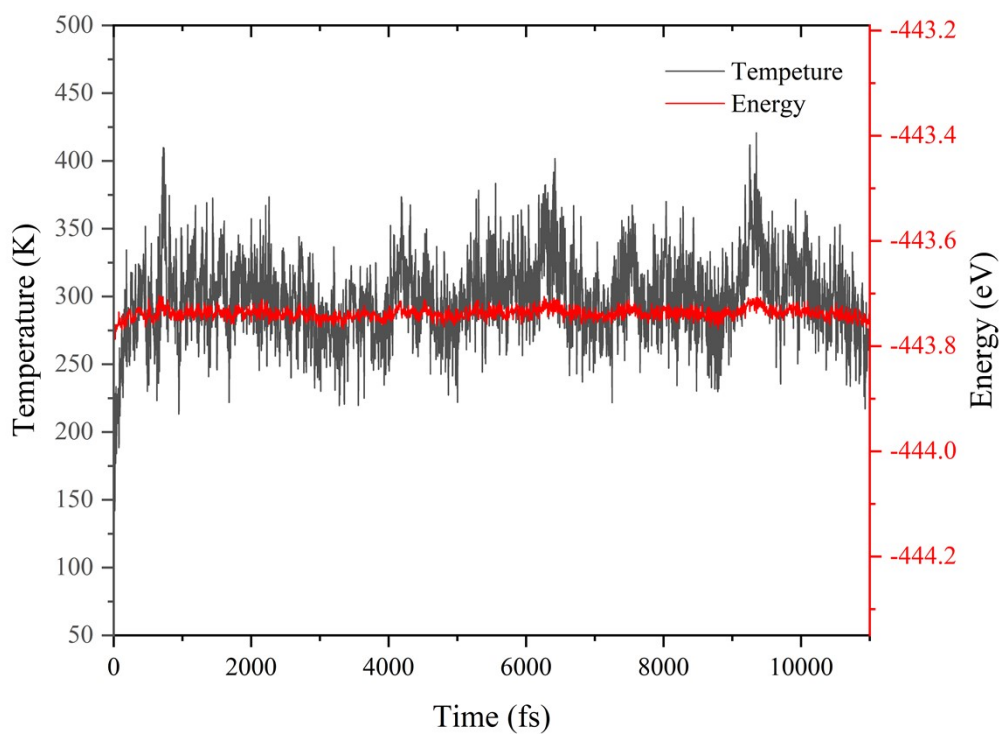


Figure S11. Energy and temperature profiles of the Ca-N₂-DV-1 structure during AIMD simulations at 300 K. The simulation consists of a 1 ps temperature control phase followed by a 10 ps equilibrium phase.

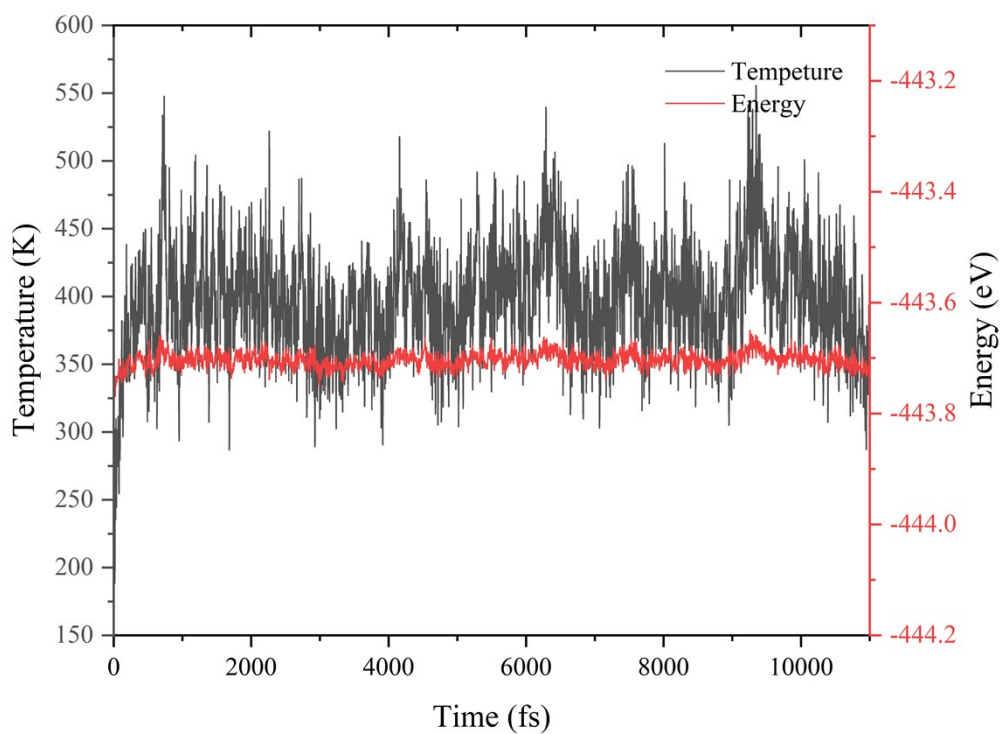


Figure S12. Energy and temperature profiles of the Ca-N₂-DV-1 structure during AIMD simulations at 400 K. The simulation consists of a 1 ps temperature control phase followed by a 10 ps equilibrium phase.

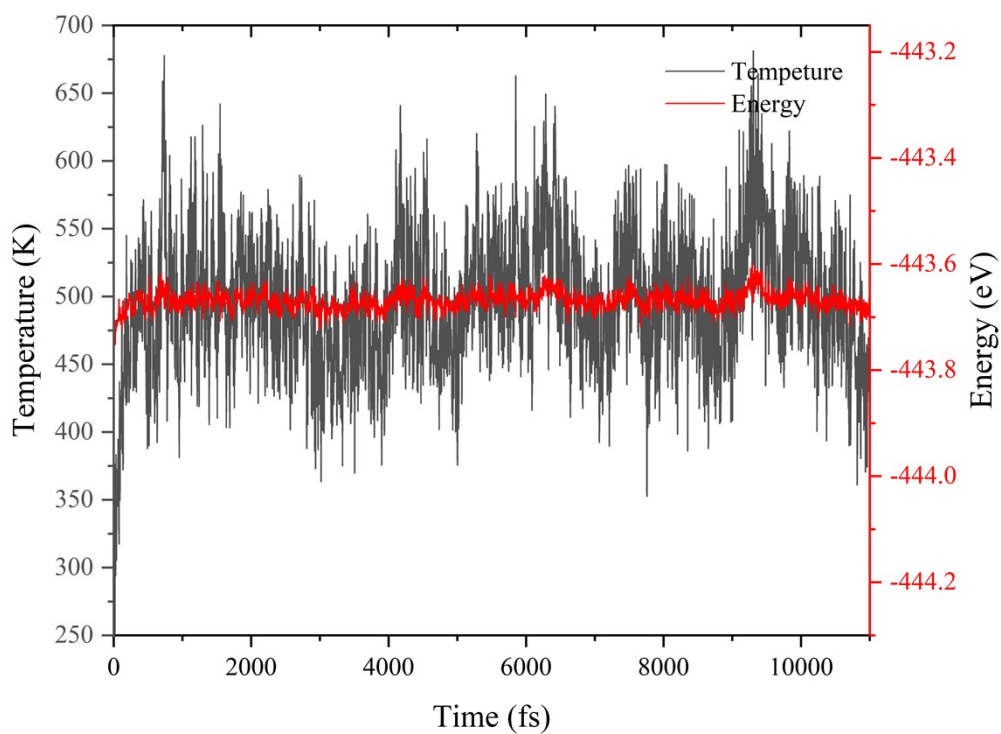


Figure S13. Energy and temperature profiles of the Ca-N₂-DV-1 structure during AIMD simulations at 500 K. The simulation consists of a 1 ps temperature control phase followed by a 10 ps equilibrium phase.

Table S1. Computed gas phase properties.

Gas molecule	Fugacity (Pa) ³	ZPE (eV)	$\int C_p dT$ (eV)	-TS (eV)
CO	101325	0.13	0.09	-0.61
CO ₂	101325	0.31	0.10	-0.66
HCOOH	3534	0.88	0.11	-0.86
H ₂ O	19	0.57	0.10	-0.27

Table S2. Thermodynamic energy corrections for selected adsorbates.

Adsorbate	ZPE (eV)	$\int C_p dT$ (eV)	-TS (eV)
*CO ₂	0.31	0.05	-0.10
*COOH	0.56	0.05	-0.11
*HCOO	0.59	0.07	-0.14
*CO	0.16	0.03	-0.05
*HCOOH	0.93	0.13	-0.28

Table S3 Calculated equilibrium potentials for electrochemical CO₂ reduction for CO and HCOOH

Reaction	Equilibrium potential (V vs RHE, pH = 6.8)
$\text{CO}_2 + 2\text{H}^+ + 2\text{e}^- \rightarrow \text{CO} + \text{H}_2\text{O}$	-0.12
$\text{CO}_2 + 2\text{H}^+ + 2\text{e}^- \rightarrow \text{HCOOH}$	-0.20

Table S4. Calculated Bader charge populations of the active sites (M) and CO₂. Geometric parameter of adsorbed CO₂.

Structure	M (slab) (e)	M (*CO₂) (e)	CO₂ (*CO₂) (e)	L_{C-O1} (Å)	L_{C-O2} (Å)	Bond angle (degree)
Mg-N ₄ -DV	8.24	8.25	16.01	1.177	1.177	179.63
Mg-N ₃ -DV	8.27	8.26	16.01	1.176	1.178	179.83
Mg-N ₃ -SV	8.17	8.26	16.92	1.260	1.260	127.11
Ca-N ₄ -DV	8.37	8.36	16.01	1.176	1.176	179.14
Ca-N ₃ -DV	8.38	8.38	16.01	1.176	1.177	178.86
Ca-N ₂ -DV-1	8.37	8.36	16.02	1.176	1.177	178.74
Ca-N ₂ -DV-2	8.42	8.41	16.01	1.176	1.177	178.87
Ca-N ₃ -SV	8.31	8.34	16.81	1.241	1.242	135.78
Ca-GY	8.26	8.30	16.86	1.262	1.263	128.31

Table S5. Calculated Bader charge populations of the active sites (M) and adsorbates (*COOH/*HCOO).

Structure	M (*COOH) (e)	COOH(*COOH) (e)	M (*HCOO) (e)	HCOO(*HCOO) (e)
Mg-N ₄ -DV	8.34	17.81	8.27	17.90
Mg-N ₃ -DV	8.36	17.78	8.31	17.90
Mg-N ₃ -SV	8.22	17.91	8.24	17.91
Ca-N ₄ -DV	8.42	17.84	8.40	17.88
Ca-N ₃ -DV	8.41	17.82	8.39	17.87
Ca-N ₂ -DV-1	8.36	17.82	8.35	17.87
Ca-N ₂ -DV-2	8.43	17.71	8.41	17.87
Ca-N ₃ -SV	8.35	17.84	8.34	17.88
Ca-GY	8.33	17.80	8.31	17.84

Table S6. Calculated Bader charge populations of the active sites (M) and adsorbates (*CO/*HCOOH).

Structure	M (*CO) (e)	CO(*CO) (e)	M (*HCOOH) (e)	HCOOH(*HCOOH) (e)
Mg-N ₄ -DV	8.30	9.99	8.30	17.96
Mg-N ₃ -DV	8.32	10.08	8.31	17.98
Mg-N ₃ -SV	8.19	10.01	8.23	17.95
Ca-N ₄ -DV	8.38	9.97	8.40	17.96
Ca-N ₃ -DV	8.41	9.98	8.42	17.96
Ca-N ₂ -DV-1	8.40	9.98	8.40	17.97
Ca-N ₂ -DV-2	8.41	10.05	8.44	18.01
Ca-N ₃ -SV	8.34	9.97	8.36	17.95
Ca-GY	8.28	9.96	8.30	17.93

Table S7. Key structural and electronic properties of the studied SACs: Bader charges population of metal sites and the M-CA bond lengths (M refers to the metal sites Mg or Ca, CA refers to the coordinating atoms C or N).

Structure	Bader charge (e)	M-CA bond length (Å)
Mg-N ₄ -DV	8.24	1.96; 1.96; 1.96; 1.96
Mg-N ₃ -DV	8.27	1.98; 1.95; 1.98; 1.97
Mg-N ₃ -SV	8.17	1.94; 1.94; 1.94
Ca-N ₄ -DV	8.37	2.27; 2.27; 2.27; 2.27
Ca-N ₃ -DV	8.38	2.32; 2.29; 2.29; 2.34
Ca-N ₂ -DV-1	8.37	2.38; 2.28; 2.28; 2.38
Ca-N ₂ -DV-2	8.42	2.31; 2.39; 2.30; 2.40
Ca-N ₃ -SV	8.31	2.19; 2.18; 2.19
Ca-GY	8.26	2.48; 2.54; 2.65; 2.65; 2.48; 2.54

Table S8. Net Charge, E_{DFT} , E_{f} , fermishift, corresponding U and potential-dependent electrochemical energy for Ca-N₄-DV with different adsorptions.

Adsorption	Net Charge (e)	E_{DFT} (eV)	E_{f} (eV)	$E_{\text{fermishift}}$ (eV)	U (V vs SHE)	E (eV)
None	1	-651.856	-2.885	0.173	-1.728	-648.971
	0.5	-650.314	-3.244	0.173	-1.369	-648.691
	0	-648.553	-3.741	0.173	-0.873	-648.553
	-0.5	-646.604	-4.058	0.173	-0.555	-648.632
	-1	-644.512	-4.306	0.173	-0.307	-648.818
CO ₂	1	-675.108	-2.861	0.177	-1.756	-672.247
	0.5	-673.577	-3.225	0.177	-1.392	-671.965
	0	-671.825	-3.721	0.177	-0.896	-671.825
	-0.5	-669.884	-4.045	0.177	-0.572	-671.907
	-1	-667.797	-4.301	0.177	-0.316	-672.098
*COOH	1	-677.400	-3.570	0.177	-1.047	-673.829
	0.5	-675.533	-3.886	0.177	-0.731	-673.59
	0	-673.519	-4.155	0.177	-0.462	-673.519
	-0.5	-671.375	-4.453	0.177	-0.164	-673.601
	-1	-669.057	-4.763	0.177	0.146	-673.819
*HCOO	1	-679.162	-3.5924	0.177	-1.025	-675.569
	0.5	-677.284	-3.9098	0.177	-0.707	-675.329
	0	-675.258	-4.178	0.177	-0.439	-675.258
	-0.5	-673.103	-4.470	0.177	-0.147	-675.338
	-1	-670.780	-4.7763	0.177	0.159	-675.556
*CO	1	-666.498	-2.887	0.176	-1.729	-663.612
	0.5	-664.955	-3.249	0.176	-1.367	-663.331
	0	-663.193	-3.740	0.176	-0.876	-663.193
	-0.5	-661.244	-4.055	0.176	-0.561	-663.272
	-1	-659.153	-4.304	0.176	-0.312	-663.458
*HCOOH	1	-682.077	-2.880	0.177	-1.737	-679.197
	0.5	-680.537	-3.246	0.177	-1.371	-678.914
	0	-678.775	-3.736	0.177	-0.881	-678.775
	-0.5	-676.828	-4.054	0.177	-0.563	-678.855
	-1	-674.736	-4.307	0.177	-0.310	-679.043

Table S9. Net Charge, E_{DFT} , E_{f} , fermishift, corresponding U and potential-dependent electrochemical energy for Ca-N₃-DV with different adsorptions.

Adsorption	Net Charge (e)	E_{DFT} (eV)	E_{f} (eV)	$E_{\text{fermishift}}$ (eV)	U (V vs SHE)	E (eV)
None	1	-650.700	-3.168	0.174	-1.446	-647.532
	0.5	-649.040	-3.473	0.174	-1.141	-647.303
	0	-647.229	-3.757	0.174	-0.857	-647.229
	-0.5	-645.277	-4.042	0.174	-0.572	-647.298
	-1	-643.170	-4.369	0.174	-0.246	-647.538
CO ₂	1	-673.930	-3.141	0.178	-1.477	-670.789
	0.5	-672.280	-3.452	0.178	-1.166	-670.554
	0	-670.477	-3.745	0.178	-0.873	-670.477
	-0.5	-668.529	-4.032	0.178	-0.586	-670.545
	-1	-666.425	-4.351	0.178	-0.267	-670.776
*COOH	1	-676.060	-3.505	0.177	-1.112	-672.555
	0.5	-674.234	-3.799	0.177	-0.818	-672.334
	0	-672.261	-4.075	0.177	-0.542	-672.261
	-0.5	-670.154	-4.376	0.177	-0.241	-672.342
	-1	-667.874	-4.710	0.177	0.093	-672.584
*HCOO	1	-677.754	-3.519	0.177	-1.098	-674.235
	0.5	-675.923	-3.8043	0.177	-0.813	-674.021
	0	-673.947	-4.0847	0.177	-0.532	-673.947
	-0.5	-671.834	-4.3896	0.177	-0.227	-674.029
	-1	-669.545	-4.7227	0.177	0.106	-674.268
*CO	1	-665.334	-3.1848	0.177	-1.432	-662.149
	0.5	-663.667	-3.4823	0.177	-1.135	-661.926
	0	-661.852	-3.7658	0.177	-0.851	-661.852
	-0.5	-659.894	-4.0594	0.177	-0.558	-661.924
	-1	-657.774	-4.4248	0.177	-0.192	-662.199
*HCOOH	1	-680.968	-3.179	0.177	-1.439	-677.789
	0.5	-679.301	-3.484	0.177	-1.134	-677.559
	0	-677.483	-3.770	0.177	-0.847	-677.483
	-0.5	-675.524	-4.059	0.177	-0.558	-677.553
	-1	-673.408	-4.381	0.177	-0.236	-677.789

Table S10. Net Charge, E_{DFT} , E_{f} , fermishift, corresponding U and potential-dependent electrochemical energy for Ca-N₂-DV-1 with different adsorptions.

Adsorption	Net Charge (e)	E_{DFT} (eV)	E_{f} (eV)	$E_{\text{fermishift}}$ (eV)	U (V vs SHE)	E (eV)
None	1	-649.944	-3.050	0.174	-1.564	-646.894
	0.5	-648.348	-3.329	0.174	-1.285	-646.683
	0	-646.609	-3.610	0.174	-1.004	-646.609
	-0.5	-644.726	-3.898	0.174	-0.716	-646.675
	-1	-642.681	-4.279	0.174	-0.336	-646.96
CO ₂	1	-673.224	-3.035	0.178	-1.584	-670.189
	0.5	-671.635	-3.310	0.178	-1.308	-669.981
	0	-669.906	-3.593	0.178	-1.025	-669.906
	-0.5	-668.032	-3.895	0.178	-0.723	-669.979
	-1	-665.982	-4.340	0.178	-0.278	-670.322
*COOH	1	-675.949	-3.437	0.178	-1.181	-672.512
	0.5	-674.154	-3.744	0.178	-0.874	-672.282
	0	-672.210	-4.031	0.178	-0.587	-672.21
	-0.5	-670.118	-4.352	0.178	-0.266	-672.294
	-1	-667.847	-4.714	0.178	0.096	-672.561
*HCOO	1	-677.723	-3.4565	0.178	-1.162	-674.266
	0.5	-675.919	-3.7591	0.178	-0.859	-674.04
	0	-673.968	-4.0413	0.178	-0.577	-673.968
	-0.5	-671.873	-4.3573	0.178	-0.261	-674.052
	-1	-669.600	-4.7121	0.178	0.094	-674.312
*CO	1	-664.617	-3.0579	0.177	-1.559	-661.559
	0.5	-663.017	-3.3349	0.177	-1.282	-661.35
	0	-661.276	-3.6151	0.177	-1.002	-661.276
	-0.5	-659.390	-3.9034	0.177	-0.714	-661.342
	-1	-657.344	-4.2832	0.177	-0.334	-661.628
*HCOOH	1	-680.198	-3.045	0.178	-1.573	-677.153
	0.5	-678.605	-3.316	0.178	-1.302	-676.947
	0	-676.872	-3.597	0.178	-1.021	-676.872
	-0.5	-674.998	-3.890	0.178	-0.728	-676.943
	-1	-672.950	-4.345	0.178	-0.273	-677.295

Table S11. Net Charge, E_{DFT} , E_{f} , fermishift, corresponding U and potential-dependent electrochemical energy for Ca-N₂-DV-2 with different adsorptions.

Adsorption	Net Charge (e)	E_{DFT} (eV)	E_{f} (eV)	$E_{\text{fermishift}}$ (eV)	U (V vs SHE)	E (eV)
None	1	-649.488	-3.223	0.174	-1.391	-646.265
	0.5	-647.798	-3.514	0.174	-1.100	-646.041
	0	-645.942	-3.882	0.174	-0.732	-645.942
	-0.5	-643.859	-4.380	0.174	-0.234	-646.049
	-1	-641.568	-4.779	0.174	0.165	-646.347
CO ₂	1	-672.717	-3.189	0.178	-1.429	-669.528
	0.5	-671.043	-3.486	0.178	-1.132	-669.299
	0	-669.200	-3.858	0.178	-0.761	-669.2
	-0.5	-667.131	-4.355	0.178	-0.263	-669.308
	-1	-664.899	-4.665	0.178	0.047	-669.565
*COOH	1	-674.819	-3.628	0.178	-0.991	-671.191
	0.5	-672.945	-3.881	0.178	-0.737	-671.004
	0	-670.925	-4.257	0.178	-0.361	-670.925
	-0.5	-668.726	-4.535	0.178	-0.083	-670.994
	-1	-666.399	-4.773	0.178	0.155	-671.172
*HCOO	1	-676.468	-3.5073	0.178	-1.111	-672.961
	0.5	-674.641	-3.7961	0.178	-0.822	-672.743
	0	-672.635	-4.2563	0.178	-0.362	-672.635
	-0.5	-670.392	-4.6412	0.178	0.023	-672.712
	-1	-667.996	-4.9533	0.178	0.335	-672.949
*CO	1	-664.428	-3.19	0.177	-1.427	-661.238
	0.5	-662.757	-3.4877	0.177	-1.129	-661.013
	0	-660.895	-3.9698	0.177	-0.647	-660.895
	-0.5	-658.765	-4.4596	0.177	-0.157	-660.995
	-1	-656.438	-4.8434	0.177	0.226	-661.281
*HCOOH	1	-679.894	-3.288	0.260	-1.412	-676.606
	0.5	-678.171	-3.586	0.260	-1.114	-676.379
	0	-676.279	-3.958	0.260	-0.742	-676.279
	-0.5	-674.154	-4.458	0.260	-0.242	-676.383
	-1	-671.824	-4.853	0.260	0.153	-676.677

Table S12. Net Charge, E_{DFT} , E_{f} , fermishift, corresponding U and potential-dependent electrochemical energy for Ca-N₃-SV with different adsorptions.

Adsorption	Net Charge (e)	E_{DFT} (eV)	E_{f} (eV)	$E_{\text{fermishift}}$ (eV)	U (V vs SHE)	E (eV)
None	1	-661.557	-2.652	0.176	-1.964	-658.904
	0.5	-660.161	-2.929	0.176	-1.687	-658.696
	0	-658.616	-3.220	0.176	-1.396	-658.616
	-0.5	-656.911	-3.549	0.176	-1.068	-658.686
	-1	-654.982	-4.334	0.176	-0.282	-659.317
CO ₂	1	-684.157	-3.175	0.180	-1.445	-680.982
	0.5	-682.475	-3.499	0.180	-1.121	-680.725
	0	-680.613	-3.869	0.180	-0.751	-680.613
	-0.5	-678.522	-4.439	0.180	-0.181	-680.742
	-1	-676.234	-4.730	0.180	0.110	-680.964
*COOH	1	-687.639	-3.157	0.180	-1.463	-684.482
	0.5	-685.965	-3.487	0.180	-1.133	-684.222
	0	-684.070	-4.241	0.180	-0.379	-684.07
	-0.5	-681.878	-4.569	0.180	-0.051	-684.162
	-1	-679.536	-4.819	0.180	0.199	-684.355
*HCOO	1	-689.336	-3.1383	0.180	-1.482	-686.198
	0.5	-687.672	-3.4691	0.180	-1.151	-685.937
	0	-685.780	-4.272	0.180	-0.348	-685.78
	-0.5	-683.504	-4.7957	0.180	0.176	-685.901
	-1	-681.037	-5.0947	0.180	0.475	-686.132
*CO	1	-676.263	-2.6458	0.179	-1.973	-673.617
	0.5	-674.874	-2.9186	0.179	-1.700	-673.415
	0	-673.334	-3.2091	0.179	-1.410	-673.334
	-0.5	-671.635	-3.5379	0.179	-1.081	-673.404
	-1	-669.711	-4.3318	0.179	-0.287	-674.042
*HCOOH	1	-691.724	-2.6513	0.179	-1.968	-689.073
	0.5	-690.328	-2.9296	0.179	-1.689	-688.864
	0	-688.783	-3.2212	0.179	-1.398	-688.783
	-0.5	-687.078	-3.5507	0.179	-1.068	-688.853
	-1	-685.147	-4.3419	0.179	-0.277	-689.489

Table S13. Net Charge, E_{DFT} , E_{f} , fermishift, corresponding U and potential-dependent electrochemical energy for Ca-GY with different adsorptions.

Adsorption	Net Charge (e)	E_{DFT} (eV)	E_{f} (eV)	$E_{\text{fermishift}}$ (eV)	U (V vs SHE)	E (eV)
None	1	-423.581	-3.5493	0.137	-1.028	-420.031
	0.5	-421.747	-3.7872	0.137	-0.790	-419.853
	0	-419.791	-4.0281	0.137	-0.549	-419.791
	-0.5	-417.712	-4.2828	0.137	-0.294	-419.854
	-1	-415.503	-4.5473	0.137	-0.030	-420.051
CO ₂	1	-445.5	-3.8991	0.141	-0.682	-441.601
	0.5	-443.484	-4.1568	0.141	-0.424	-441.406
	0	-441.337	-4.4257	0.141	-0.155	-441.337
	-0.5	-439.055	-4.68	0.141	0.099	-441.395
	-1	-436.653	-4.9128	0.141	0.332	-441.566
*COOH	1	-449.209	-3.8587	0.141	-0.722	-445.35
	0.5	-447.212	-4.1179	0.141	-0.463	-445.153
	0	-445.083	-4.3895	0.141	-0.192	-445.083
	-0.5	-442.813	-4.6773	0.141	0.096	-445.151
	-1	-440.392	-4.9737	0.141	0.393	-445.366
*HCOO	1	-450.803	-3.8839	0.141	-0.697	-446.919
	0.5	-448.794	-4.1425	0.141	-0.439	-446.723
	0	-446.653	-4.4133	0.141	-0.168	-446.653
	-0.5	-444.37	-4.7016	0.141	0.121	-446.721
	-1	-441.93	-5.4271	0.141	0.846	-447.357
*CO	1	-438.227	-3.5272	0.140	-1.053	-434.7
	0.5	-436.405	-3.7629	0.140	-0.817	-434.524
	0	-434.461	-4.0059	0.140	-0.574	-434.461
	-0.5	-432.393	-4.2623	0.140	-0.318	-434.524
	-1	-430.194	-4.5283	0.140	-0.052	-434.722
*HCOOH	1	-453.603	-3.5173	0.141	-1.064	-450.086
	0.5	-451.786	-3.7526	0.141	-0.828	-449.909
	0	-449.847	-3.9949	0.141	-0.586	-449.847
	-0.5	-447.784	-4.2509	0.141	-0.330	-449.909
	-1	-445.591	-4.5169	0.141	-0.064	-450.108

Table S14. Net Charge, E_{DFT} , E_{f} , fermishift, corresponding U and potential-dependent electrochemical energy for Mg-N₄-DV with different adsorptions.

Adsorption	Net Charge (e)	E_{DFT} (eV)	E_{f} (eV)	$E_{\text{fermishift}}$ (eV)	U (V vs SHE)	E (eV)
None	1	-676.711	-3.820	0.250	-1.653	-647.531
	0.5	-674.719	-4.137	0.250	-1.283	-647.245
	0	-672.584	-4.390	0.250	-0.816	-647.111
	-0.5	-670.329	-4.659	0.250	-0.506	-647.186
	-1	-667.918	-4.940	0.250	-0.259	-647.368
CO ₂	1	-674.069	-3.063	0.260	-1.637	-671.005
	0.5	-672.436	-3.433	0.260	-1.267	-670.719
	0	-670.578	-3.955	0.260	-0.745	-670.578
	-0.5	-668.521	-4.275	0.260	-0.425	-670.658
	-1	-666.322	-4.518	0.260	-0.182	-670.84
*COOH	1	-676.711	-3.820	0.260	-0.880	-672.892
	0.5	-674.719	-4.137	0.260	-0.563	-672.651
	0	-672.584	-4.390	0.260	-0.310	-672.584
	-0.5	-670.329	-4.659	0.260	-0.041	-672.658
	-1	-667.918	-4.940	0.260	0.240	-672.858
*HCOO	1	-678.148	-3.7489	0.260	-0.951	-674.399
	0.5	-676.189	-4.0681	0.260	-0.632	-674.155
	0	-674.085	-4.3305	0.260	-0.370	-674.085
	-0.5	-671.858	-4.6089	0.260	-0.091	-674.162
	-1	-669.469	-4.903	0.260	0.203	-674.372
*CO	1	-665.184	-3.1082	0.260	-1.592	-662.076
	0.5	-663.530	-3.4766	0.260	-1.223	-661.792
	0	-661.653	-3.9798	0.260	-0.720	-661.653
	-0.5	-659.584	-4.2964	0.260	-0.404	-661.732
	-1	-657.373	-4.5422	0.260	-0.158	-661.916
*HCOOH	1	-681.041	-3.073	0.260	-1.627	-677.968
	0.5	-679.403	-3.449	0.260	-1.251	-677.678
	0	-677.534	-3.982	0.260	-0.718	-677.534
	-0.5	-675.464	-4.303	0.260	-0.397	-677.616
	-1	-673.257	-4.530	0.260	-0.170	-677.787

Table S15. Net Charge, E_{DFT} , E_{f} , fermishift, corresponding U and potential-dependent electrochemical energy for Mg-N₃-DV with different adsorptions.

Adsorption	Net Charge (e)	E_{DFT} (eV)	E_{f} (eV)	$E_{\text{fermishift}}$ (eV)	U (V vs SHE)	E (eV)
None	1	-649.268	-3.355	0.250	-1.335	-645.913
	0.5	-647.517	-3.650	0.250	-1.041	-645.692
	0	-645.621	-3.926	0.250	-0.764	-645.621
	-0.5	-643.586	-4.218	0.250	-0.473	-645.694
	-1	-641.389	-4.574	0.250	-0.116	-645.963
CO ₂	1	-673.142	-3.380	0.260	-1.320	-669.762
	0.5	-671.372	-3.692	0.260	-1.008	-669.526
	0	-669.451	-3.974	0.260	-0.726	-669.451
	-0.5	-667.392	-4.271	0.260	-0.429	-669.527
	-1	-665.169	-4.608	0.260	-0.092	-669.777
*COOH	1	-675.438	-3.8572	0.260	-0.843	-671.581
	0.5	-673.436	-4.1447	0.260	-0.555	-671.364
	0	-671.278	-4.4789	0.260	-0.221	-671.278
	-0.5	-668.836	-5.0898	0.260	0.390	-671.381
	-1	-666.200	-5.4293	0.260	0.729	-671.63
*HCOO	1	-677.030	-3.7874	0.260	-0.913	-673.242
	0.5	-675.058	-4.0878	0.260	-0.612	-673.014
	0	-672.919	-4.4843	0.260	-0.216	-672.919
	-0.5	-670.448	-5.1815	0.260	0.481	-673.038
	-1	-667.770	-5.5218	0.260	0.822	-673.292
*CO	1	-664.370	-3.5119	0.260	-1.188	-660.858
	0.5	-662.537	-3.8147	0.260	-0.885	-660.63
	0	-660.561	-4.0795	0.260	-0.621	-660.561
	-0.5	-658.467	-4.3440	0.260	-0.356	-660.639
	-1	-656.211	-4.6824	0.260	-0.018	-660.894
*HCOOH	1	-679.625	-3.394	0.260	-1.306	-676.232
	0.5	-677.852	-3.692	0.260	-1.008	-676.006
	0	-675.932	-3.975	0.260	-0.725	-675.932
	-0.5	-673.870	-4.278	0.260	-0.422	-676.009
	-1	-671.636	-4.664	0.260	-0.036	-676.301

Table S16. Net Charge, E_{DFT} , E_{f} , fermishift, corresponding U and potential-dependent electrochemical energy for Mg-N₃-SV with different adsorptions.

Adsorption	Net Charge (e)	E_{DFT} (eV)	E_{f} (eV)	$E_{\text{fermishift}}$ (eV)	U (V vs SHE)	E (eV)
None	1	-661.203	-2.757	0.255	-1.938	-658.446
	0.5	-659.755	-3.033	0.255	-1.663	-658.239
	0	-658.159	-3.323	0.255	-1.372	-658.159
	-0.5	-656.403	-3.651	0.255	-1.044	-658.228
	-1	-654.425	-4.423	0.255	-0.272	-658.848
CO ₂	1	-682.848	-3.386	0.265	-1.319	-679.462
	0.5	-681.082	-3.665	0.265	-1.040	-679.25
	0	-679.095	-4.453	0.265	-0.252	-679.095
	-0.5	-676.717	-4.988	0.265	0.283	-679.211
	-1	-674.160	-5.248	0.265	0.543	-679.409
*COOH	1	-686.677	-3.278	0.265	-1.427	-683.4
	0.5	-684.944	-3.608	0.265	-1.097	-683.14
	0	-682.984	-4.399	0.265	-0.306	-682.984
	-0.5	-680.689	-4.752	0.265	0.047	-683.065
	-1	-678.255	-4.993	0.265	0.288	-683.249
*HCOO	1	-688.224	-3.2919	0.265	-1.413	-684.932
	0.5	-686.483	-3.6246	0.265	-1.080	-684.671
	0	-684.514	-4.4167	0.265	-0.288	-684.514
	-0.5	-682.157	-4.9694	0.265	0.264	-684.642
	-1	-679.602	-5.278	0.265	0.573	-684.88
*CO	1	-675.492	-3.1378	0.262	-1.965	-672.316
	0.5	-673.850	-3.4343	0.262	-1.686	-672.106
	0	-672.047	-3.7439	0.262	-1.394	-672.025
	-0.5	-670.076	-4.0902	0.262	-1.065	-672.095
	-1	-667.874	-4.8794	0.262	-0.283	-672.723
*HCOOH	1	-690.509	-2.781	0.265	-1.924	-687.728
	0.5	-689.049	-3.057	0.265	-1.649	-687.521
	0	-687.441	-3.345	0.265	-1.360	-687.441
	-0.5	-685.675	-3.672	0.265	-1.033	-687.511
	-1	-683.687	-4.450	0.265	-0.256	-688.136

Reference

1. Richard Dronskowski, Peter E. Bloechl. Crystal orbital Hamilton populations (COHP): energy-resolved visualization of chemical bonding in solids based on density-functional calculations. *J. Phys. Chem.* **1993**, 97(33), 8617–8624. DOI:10.1021/j100135a014
2. Nelson R, Ertural C, George J, Deringer VL, Hautier G, Dronskowski R. LOBSTER: Local orbital projections, atomic charges, and chemical-bonding analysis from projector-augmented-wave-based density-functional theory. *J Comput Chem.* **2020**, 41(21), 1931-1940. DOI:10.1002/jcc.26353
3. Yan Jiao, Yao Zheng, Ping Chen, Mietek Jaroniec, Shi-Zhang Qiao. Molecular Scaffolding Strategy with Synergistic Active Centers To Facilitate Electrocatalytic CO₂ Reduction to Hydrocarbon/Alcohol. *J. Am. Chem. Soc.* **2017**, 139(49), 18093–18100. DOI:10.1021/jacs.7b10817